MAGNETIC PLATFORMS BASED ON MAGNETITE AND POLYPHENOLS WITH ANTIMICROBIAL ACTIVITY

Cornelia-Ioana ILIE[1,2], Angela SPOIALĂ[1,2], Denisa FICAI[2,3], Adrian-Ionuț NICOARĂ[1,2], Ovidiu-Cristian OPREA[2-4], Vasile-Adrian SURDU[1,2], Roxana Doina TRUȘCĂ[2], Ecaterina ANDRONESCU[1,2,4], Lia-Mara DIȚU[5,6], Anton FICAI[1,2,4,*]

This study synthesised magnetic drug delivery systems through spraying assisted coprecipitation method. The manuscript aimed to develop innovative drug delivery systems based on magnetite nanoparticles loaded with polyphenols. The as-obtained nano-drugs were morphologically and structurally characterised by Fourier transform infrared spectroscopy (FTIR), X-ray diffraction (XRD), vibrating sample magnetometer (VSM), scanning electron microscopy (SEM), thermogravimetric analysis (TGA) and by determining the antibacterial activity. The XRD pattern showed the characteristic peaks of tetrahedral and polyhedral magnetite crystals, specifying that magnetic nanocarriers presented high crystallinity. The crystallite size of magnetic nanoparticles synthesised is 7.3-8.2nm, according to the microscopic data. The antibacterial activity of nanocarriers tested makes their potential for use in biomedical applications.

Keywords: magnetic nanoparticles, polyphenols, drug delivery systems, antimicrobial agents

1. Introduction

Nanotechnology and nanomedicine have been working together to develop and improve the effectiveness of various drugs. Therefore, through nanotechnology, scientists could understand and use nanomaterials the nanomedicine. For the past few decades, medical research has focused on

[1] Department of Science and Engineering of Oxide Materials and Nanomaterials, Faculty of Chemical Engineering and Biotechnologies, University POLITEHNICA of Bucharest, Romania; cornelia_ioana.ilie@upb.ro, angela.spoiala@upb.ro, adrian.nicoara@upb.ro, adrian.surdu@upb.ro, ecaterina.andronescu@upb.ro, *Correspondence: anton.ficai@upb.ro

[2] National Centre for Micro and Nanomaterials and National Centre for Food Safety, Faculty of Chemical Engineering and Biotechnologies, University POLITEHNICA of Bucharest, Romania; truscaroxana@yahoo.com

[3] Department of Inorganic Chemistry, Physical Chemistry and Electrochemistry, Faculty of Chemical Engineering and Biotechnologies, University POLITEHNICA of Bucharest, Romania; ovidiu73@yahoo.com, denisaficai@yahoo.ro

[4] Academy of Romanian Scientists, Bucharest, Romania

[5] Department of Microbiology and Immunology, Faculty of Biology, University of Bucharest, Bucharest, Romania; lia-mara.ditu@bio.unibuc.ro

[6] Department of Microbiology and Immunology, Faculty of Biology& Research Institute of the University of Bucharest, Bucharest, Romania

developing new drugs and delivery system platforms to improve their efficient delivery and increase the quality of life of those patients [1]. Nanoparticles are essential nanomaterials used in various biomedical applications, such as medical diagnosis, regenerative medicine, antitumoral therapy, and drug delivery [2-7]. Thus, nanomaterials have been investigated for nano-drug applications, such as quantum dots (metals, oxides, etc.), dendrimers, lipids, liposomes, and polymer nanoparticles. Using nano-drugs based on nanoparticles for developing drug delivery platforms represents the "milestone" for nanomedicine [8-10].

Polyphenols have attracted great interest in medicine, food, and cosmetics due to their versatile functionalities and the high interest in developing such innovative nano-drugs delivery systems. Epidemiologists consider polyphenols as many bioactive substances from plant foods that have a key role in human health. Researchers have discovered that polyphenols are essential in preventing degenerative diseases, such as cancers and cardiovascular and neurodegenerative diseases [11]. Also, polyphenols have been found to act as co-oxidants and possess a vital role in regenerating essential vitamins [12]. After studying its structure, it was found that polyphenolic compounds have pharmacological properties such as antioxidative, antitumoral, anti-inflammatory [13], anti-mutagenic, anti-carcinogenic [14], and anti-diabetic [15], and anti-ageing properties [16].

Gallic acid is a polyphenol usually found in strawberries, grapes, bananas, lemons, chocolate, and wine [17, 18]. Due to its low cytotoxic effect on healthy cells and high toxicity against cancerous cells, it is considered an important natural bioactive food compound [17, 19, 20]. Gallic acid has been used against different cancers such as prostate cancer, lung cancer, breast cancer, gastric cancer, colon cancer, cervical cancer, melanoma, oesophageal cancer [17, 21, 22], pancreatic cancer [23], and brain tumours [20, 24]. Another important polyphenol, caffeic acid, is naturally found in coffee, fruits, plants, oils, grapes, and tea; it is a hydroxycinnamic acid characterised by strong antioxidant power due to radical scavenging activity and the inhibition of lipid peroxidation. However, the poor water solubility and chemical stability of caffeic acid make necessary the use of specialised delivery systems suitable for its solubilisation, protection from degradation, and the maintenance of its antioxidative activity for a longer time [25, 26]. Both polyphenols present anti-inflammatory and anti-diabetic [24], antiangiogenic and anti-melanogenic [19], antibacterial [27], antiviral [17, 27], antifungal [17], antiulcer [17, 24], anti-mutagenic effects [18] and wound healing capacity [28].

Researchers have recently focused on the development and *in vitro and in vivo* application of magnetic nanoparticles due to their physicochemical use as targeted drug delivery systems in biomedicine, such as hyperthermia, magnetic resonance imaging, cell tracking, theranostics, biosensors, tissue engineering etc.

[29-34]. Furthermore, magnetite (Fe_3O_4) and maghemite (γ-Fe_2O_3) with a smaller particle size of 10-20 nm are ideal for using them in biomedical applications; moreover, their functionalisation capacity enhances the amount of therapeutic agent loaded on their surface as well as their stability *in vitro* and *in vivo* [35, 36].

The present study focuses on using magnetite nanoparticles loaded with biologically active compounds to synthesise/develop a novel model of nano-drug delivery systems for biomedical applications with potential use in treating infections.

2. Material and methods

2.1. Materials

The synthesis of magnetic nanoparticles was performed using sodium hydroxide with ≥98% purity (Fluka); ammonium iron sulphate crystallised hexahydrate having ≥98% purity (Roth); iron chloride (97% reagent grade). Caffeic acid (≥98% purity) and ethanol (≥99.8%) were purchased from Sigma-Aldrich. The anhydrous trisodium citrate (99% purity) was acquired from Alfa Aesar. Silver nitrate (min. 99.5% purity) was acquired from Silal Trading. Gallic acid (≥98% purity) was obtained from Merck. All chemicals were used without further purification. The microbiological assays were performed using Nutrient Broth No. 2 and agar purchased from Sigma-Aldrich (Germany, Darmstadt). All strains studied in this paper were provided from the Microorganisms Collection of the Department of Microbiology, Faculty of Biology of the University of Bucharest.

2.2. Methods

The Fe_3O_4 nanoparticles and magnetic nanoparticles loaded with biologically active compounds were synthesised by spraying assisted coprecipitation [37] using ammonium iron sulphate hexahydrate and iron chloride as precursors, respectively, anhydrous trisodium citrate as a stabilising agent. After the Fe_3O_4@citrate magnetic nanoparticles were synthesised, they were loaded with polyphenols by grinding 100mg Fe_3O_4@citrate (nanopowder) with a solution formed by dissolving 10mg polyphenol in 1mL of ethanol. The grinding process was continued until the solvent was evaporated, and the stabilised magnetic nanoparticles loaded with polyphenols were obtained in a dry form.

The obtained nanoparticles have been characterised by XRD, FTIR, VSM, ATD, SEM and antibacterial assessments.

X-Ray Diffraction experiments were carried out on PANalytical Empyrean equipment operated at 45 kV and 40 mA in Bragg-Brentanno geometry using CuKα radiation (λ=1.5418 Å). The diffractometer was equipped with a 1/4° fixed divergent slit, 0.02° Soller slit and 1/2° anti-scatter slit on the incident beam side and 1/2° anti-scatter slit, 0.02° Soller slit, and 0.02 mm Ni filter mounted on

PIXCel3D detector on the diffracted beam side. Pulse height discrimination lower level was set at 40% to filter fluorescence contribution caused by iron ions. The parameters used during measurement were scan range 10.0000 - 80.0107° 2θ, step size of 0.0263° and counting time per step of 510s. Data reduction, search and match procedures were performed using HighScorePlus 3.0.e software and ICDD PDF4+ 2020 database.

The presence of functional groups of the magnetic nanocarrier was highlighted using a Nicolet iS50 **FTIR** spectrometer (Nicolet, MA, USA), which is equipped with a DTGS detector that provides information with high sensitivity in the range of 4000cm^{-1} to 400cm^{-1} with a resolution of 4cm^{-1} by summing up 32 scans to improve the quality of the spectra. Measurements were performed at room temperature, and the recording and analysis of the data were performed using the Omnic32 software.

The magnetic behaviour of the Fe_3O_4@citrate samples loaded with the polyphenols was evaluated with the **vibrating sample magnetometer** at 25±2°C using the 7400 Series VSM equipment manufactured by LakeShore. Data analysis was performed using the GraphPad Prism, version 9.4, provided by GraphPad Software (San Diego, CA, USA).

For **thermal analysis**, approximately 10mg of each sample was placed in an open alumina crucible in a Netzsch (Selb, Germany) STA 449C Jupiter apparatus. The heating was done from room temperature up to 900°C, with 10 K·min^{-1}, under a flow of 50mL·min^{-1} dried air. An empty alumina crucible was used as a reference.

The **SEM** images for determination of the size and morphology of the magnetic nanocarriers were recorded using a Quanta Inspect F50 (FEI Company, Eindhoven, Netherlands) scanning electron microscope equipped with field emission gun electron (FEG) with 1.2nm resolution and an energy dispersive X-ray spectrometer with an MnK resolution of 133eV.

The **antimicrobial assessments** were performed using methods from a previous study [38] and according to the CLSI standards [39]. The antimicrobial activity of magnetic nanocarriers was evaluated using qualitative and quantitative assays (diameters of the inhibitions zones and minimum inhibitory concentrations-MICs). The experiments were performed in triplicate, and the values were expressed as mean ± SD (standard deviation). The data results were statistically analysed using GraphPad Prism 9.4. The differences between groups were compared using a one-way analysis of variance (one-way ANOVA) and Tukey's multiple comparisons test. p-value < 0.05 was considered statistically significant.

3. Results and discussion

3.1. X-ray diffraction

The determination of the structure of magnetic nanoparticles was performed using X-ray diffraction, which confirmed the cubic structure of magnetite nanoparticles for all samples.

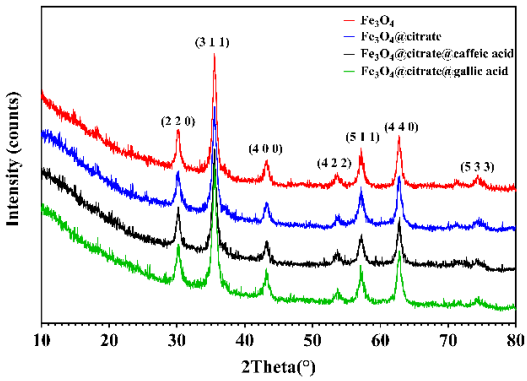

Fig. 1. XRD diagram of magnetic nanoparticles (stabilised with citrate and loaded with polyphenols)

Fig. 1 shows the characteristic peaks of tetrahedral and polyhedral magnetite crystals as follows: 30°, 35.5°, 43.2°, 53.5°, 57.2°, 63° and 74° [40-45]. Mean crystallite size and crystallinity were assessed after the whole pattern Pawley fit of X-ray diffractograms. The peak profile was estimated using a Pseudo-Voigt function, and the background was calculated as a polynomial function (Table 1).

Table 1.

Crystallite size and crystallinity for the magnetic samples

Sample	Mean crystallite size (nm)	Standard deviation	Crystallinity (%)
Fe_3O_4	7.30	4.41	19.4
Fe_3O_4@citrate	7.45	3.19	23.09
Fe_3O_4@citrate@caffeic acid	7.99	1.52	15.69
Fe_3O_4@citrate@gallic acid	7.63	2.90	16.30

The crystallite size of magnetic nanoparticles synthesised is in the range of 7.3-8.2nm. Considering that all the samples loaded with polyphenols were obtained starting from Fe_3O_4@citrate (control sample), a slight modification/increase of the dimensions of the crystallites is observed as a consequence of the loading process. Based on these data, it can be assumed that ethanol as a solvent does not alter the magnetic support and acts just as a solvent to dissolve the polyphenols during the loading.

3.2. FTIR spectroscopy

Following the FTIR analysis of magnetic nanoparticles (Fig. 2), bands characteristic of Fe-O bonds at 544cm^{-1} can be observed due to the stretching vibration associated with the absorption and corresponding to tetrahedral and polyhedral shapes crystallites [41, 44, 46]. The range of 3387-3398cm^{-1} is assigned to the stretching of associated hydroxyl groups, while at ~1636cm^{-1}, the bending vibration of the hydroxyl group can be observed. Likewise, C=C vibration of the aromatic nucleus can be found between 1500 and 1600cm^{-1}, while the 1,4 substitution of the benzene nucleus in the range 805-897cm^{-1} can be observed. Because low concentrations of trisodium citrate and polyphenols were used, it is observed that the characteristic peaks have low intensities.

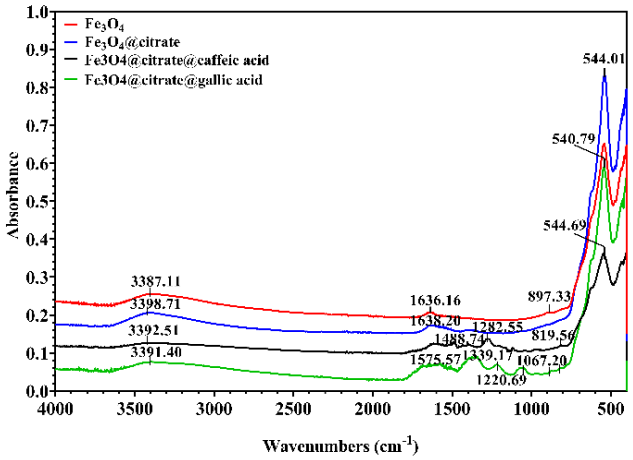

Fig. 2. FTIR analysis of magnetic powders stabilised with citrate and loaded with polyphenols

3.3. The degree of magnetisation/VSM analysis

The analysis of the degree of magnetisation is presented in Fig. 3. It confirms the characteristic behaviour of magnetite, respectively, of core@shell magnetite homologues. The magnetisation/ mass ratio of pure magnetite is 63.477emu/g, and the coercivity is 28.937Oe, respectively, for magnetite stabilised with citrate is slightly decreased to 60.772emu/g, while coercivity is 17.105Oe. In the case of the samples loaded with biological compounds, the magnetisation/ mass ratio and coercivity additionally decreased: for Fe_3O_4@caffeic acid, the magnetisation/mass is 57.379emu/g, and coercivity is 16.232Oe, for Fe_3O_4@gallic acid is 54.736emu/g, and coercivity is 14.086Oe. The magnetisation/mass ratio decrease is due to the dilution of the magnetic component along with the shielding of the shell/organic compounds (citrate and polyphenols). These results are in good agreement with other studies obtained by the coprecipitation method [41, 47, 48].

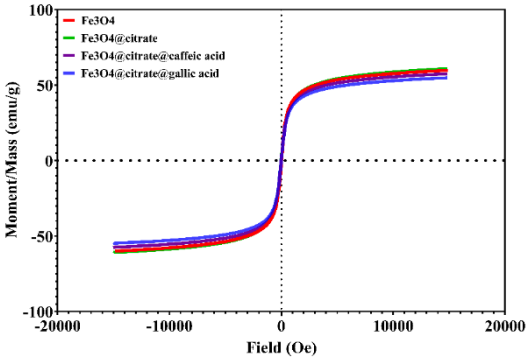

Fig. 3. Magnetisation curves of the magnetic carriers

3.4. Thermal analysis

The TG-DSC curves for magnetic nanoparticles are presented in Fig. 4, and the relevant data are centralised in Table 2.

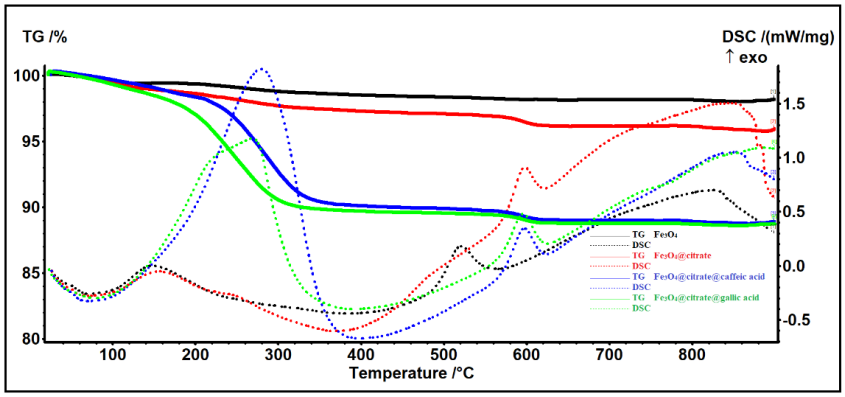

Fig. 4. The TG-DSC curves for magnetic nanoparticles loaded with phenolic compounds

Table 2.

Residual mass of samples

Sample	Temperature (°C)	Mass loss (%)	Residual Mass (%)
Fe_3O_4	<160	0.63	98.17
	160-900	1.25	
Fe_3O_4@citrate	<145	1.13	95.95
	145-545	2.01	
	545-900	1.00	
Fe_3O_4@citrate@ caffeic acid	<210	1.83	88.92
	210-400	8.14	
	400-900	1.18	
Fe_3O_4@citrate@ gallic acid	<180	2.26	88.73
	180-400	8.12	
	400-900	0.95	

For the samples coated with a stabilising agent (citrate) and polyphenols, the maghemite-hematite transformation occurs at a higher temperature because the magnetite nanoparticles are protected by the organic layer and especially by the derived carbonic residue [42, 49]. The Fe_3O_4 sample loses 0.63% of its initial mass in the RT-160°C range. At this phase, the process is accompanied by an endothermic effect with a minimum of 71.4°C, which is characteristic of the elimination of water molecules weakly bound to the surface of the nanoparticles. In the interval 160-180°C, a small mass increase is visible on the TG curve, corresponding to the oxidation of Fe^{2+} to Fe^{3+} (transformation of magnetite to maghemite) [50]. The sample continues to lose mass, more intensely up to 400°C and then slowly until the end of the analysis. Between 160-900°C, there is a mass loss of 1.25%. Most likely, it is the removal of water by condensing the existing "-OH" groups on the surface of the nanoparticles. The endothermic effect accompanies the process, with a minimum of 383.9°C. At 521.4°C, an exothermic effect is specific to magnetite samples, corresponding to the maghemite-hematite transformation [51].

Citrate-coated magnetic nanoparticles are more stable, with decomposition/ mass loss processes at higher temperatures. In the RT-145°C range, the sample eliminates the water absorbed on the particle surface, the mass loss being 1.13%. Dehydration is accompanied by an endothermic effect with a minimum of 72.9°C. Between 145-545°C, the sample loses mass continuously, 2.01%; the process is followed by an endothermic effect with a minimum of 367.3°C. At this stage, water is removed by condensing the "-OH" groups bound to the nanoparticles, and the degradation of the existing citrate in the sample begins.

Between 545-900°C, the sample loses 1.00% of its mass by oxidising the organic part. The exothermic effect at 598°C highlights the maghemite-hematite transformation. The residual mass recorded is 95.95%. The sample may have somewhere between 4-5% absorbed trisodium citrate (estimated because the citrate residue is generally a mixture).

The Fe_3O_4@citrate@caffeic acid sample loses 1.83% of the initial mass up to 210°C, an endothermic process with a minimum of 69.6°C, represented by the loss of water molecules. Between 210-400°C, the oxidative degradation of the organic part (caffeic acid) takes place, the sample losing 8.14%. The process is followed by an exothermic effect with a maximum of 279.8°C. Between 400-900°C, the sample loses another 1.18%, the residual mass being 88.92%. The maghemite-hematite transformation is visible at 597.3°C. Since the residual mass of caffeic acid is zero, the amount of caffeic acid can be estimated at 7.33%.

The Fe_3O_4@citrate@gallic acid sample eliminates 2.26% of the initial mass (water molecules) in the range of RT-180°C through a process accompanied by an endothermic effect with a minimum of 77.5°C. In the interval 180-400°C,

the organic part's oxidative degradation occurs (gallic acid), the sample losing 8.12%. The process is accompanied by an exothermic and asymmetric effect with a maximum at 269.1°C and a shoulder at 219°C. Between 400-900°C, the sample loses 0.95%, the residual mass being 88.73%. The maghemite-hematite transformation is visible at 599.5°C. Since the residual mass of gallic acid is zero, the amount of gallic acid can be estimated at 7.52%.

3.5. Scanning Electron Microscopy (SEM)

The SEM analysis obtains information about the morphology of magnetic nanoparticles. According to the results acquired from the XRD analysis, the size of the magnetite crystallites is around 7-8 nm. Still, the agglomerates can only be observed with the help of SEM analysis (Fig. 5). Also, the size of Fe_3O_4@citrate@gallic acid NPs is more than Fe_3O_4@citrate@caffeic acid NPs.

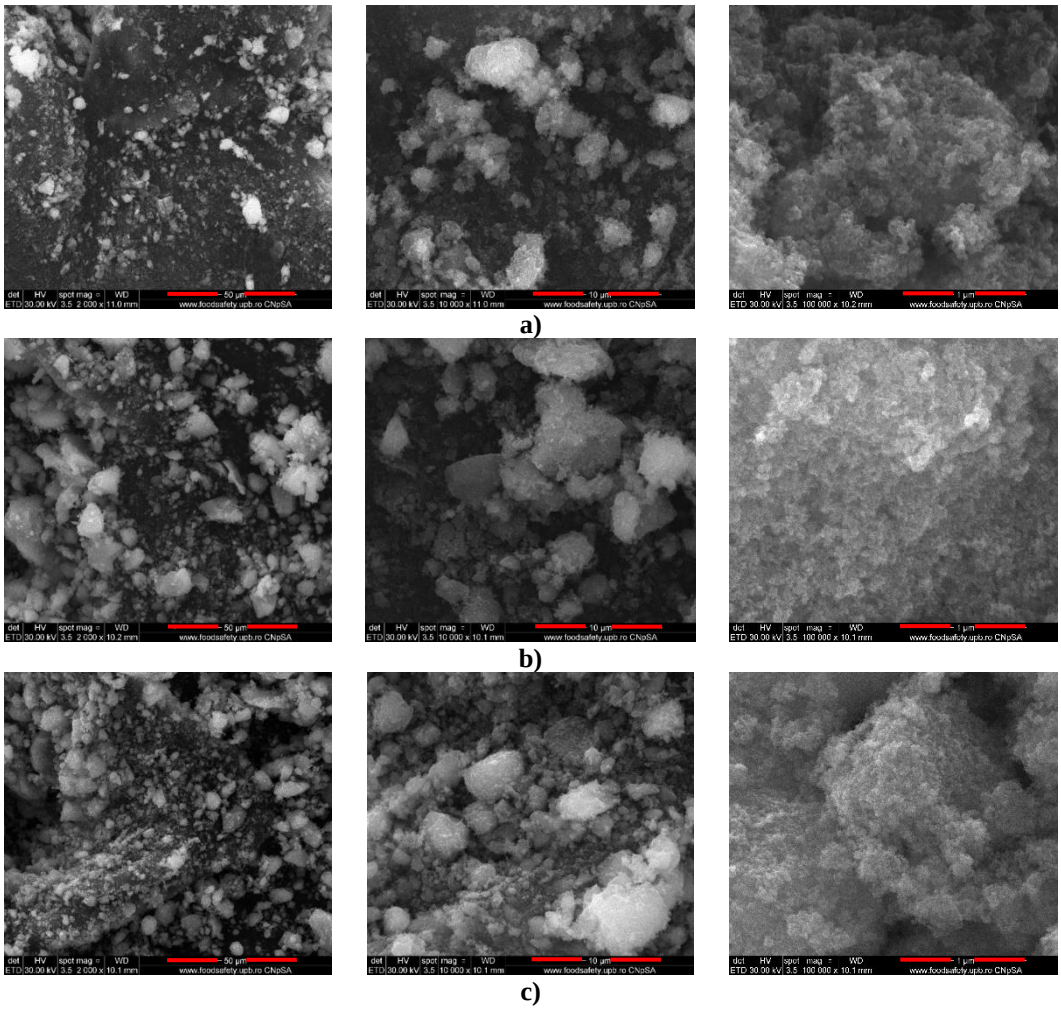

a)

b)

c)

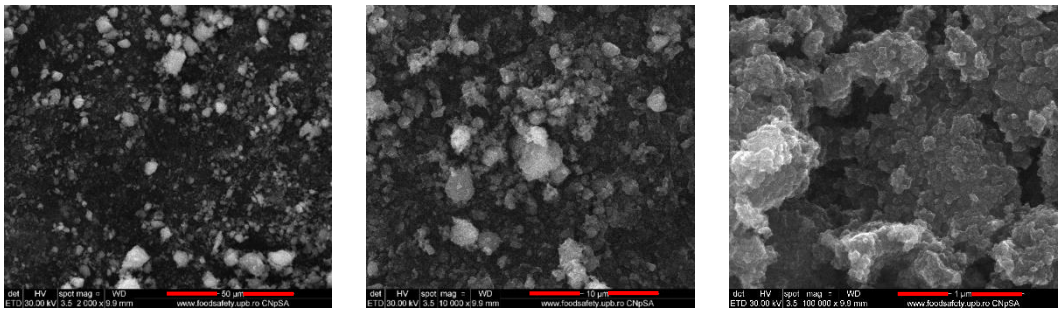

d)

Fig. 5. SEM images for samples: (a)-Fe_3O_4; (b)-Fe_3O_4@citrate; (c)-Fe_3O_4@citrate@caffeic acid; (d)-Fe_3O_4@citrate@gallic acid

3.6. Antibacterial assays

The antimicrobial activity of Fe_3O_4 NPs is due to different interactions with bacterial cells (membrane depolarisation, production of reactive oxygen species, DNA damage, mitochondrial dysfunction etc.) [35, 52]. The qualitative results indicate the antibacterial potential of magnetic nanocarriers. The samples decreased the growth of the bacterial strains tested, and controls (Fe_3O_4 and Fe_3O_4@citrate) inhibited moderate adherence of the bacterial cells on their surfaces. Table 3 shows the higher sensitivity of Gram-positive than Gram-negative bacteria for Fe_3O_4 loaded with polyphenols. Recent studies reported magnetic NP's antibacterial activity in Gram-positive and Gram-negative bacteria [53-55].

Table 3.

The diameters of the inhibition zones

Bacterial strains	**The diameter of the inhibition zone (mm) ± SD**			
	Fe_3O_4	**Fe_3O_4@ citrate**	**Fe_3O_4@citrate@ caffeic acid**	**Fe_3O_4@citrate@ gallic acid**
S. aureus ATCC 25923	2.0	2.0	6.4±0.10	5.0±0.11
E. coli ATCC 25922	2.0	2.0	4.1±0.05	4.5±0.08
P. aeruginosa ATCC 27853	2.0	2.0	3.9±0.02	4.7±0.06

The MIC values represented the lowest concentration of the tested NPs that inhibited microbial growth. The results of quantitative assays are presented below.

Table 4.

MIC values for tested Fe_3O_4 NPs

Bacterial strains	**MIC (µg/mL)**					
	Fe_3O_4	**Fe_3O_4@citrate**	**Fe_3O_4@citrate @ caffeic acid**	**caffeic acid**	**Fe_3O_4@citrate @ gallic acid**	**gallic acid**
S. aureus ATCC 25923	1.25	1.25	0.31	0.15	0.62	0.15
E. coli ATCC 25922	2.5	1.25	**0.08**	0.62	**0.15**	1.25
P. aeruginosa ATCC 27853	0.31	0.31	**0.04**	0.08	**0.04**	0.15

The qualitative results were confirmed by the quantitative analysis (MICs evaluation). The inhibitory effect of the magnetic nanocarriers was observed for all tested strains. The most sensitive strains were *E. coli* and *P. aeruginosa*. The MIC values ranged between 0.04 and 0.15 µg/mL for Fe_3O_4@citrate loaded with polyphenols. In Table 4, it can observe a synergic effect for Fe_3O_4@citrate@caffeic acid and Fe_3O_4@citrate@gallic acid between magnetic NPs and biological compounds against *E. coli* and *P. aeruginosa*. Caffeic acid-based magnetic nanocarriers have been proven to be more potent against *S. aureus* and *E. coli* and quite similar to the sample loaded with gallic acid against *P. aeruginosa*. The results were in concordance with the literature. Shah *et al.* [48] presented the antibacterial and antifungal activity of the Fe_3O_4 functionalised with gallic acid (average particle size 5-11 nm).

The bacteriostatic effect exhibited on the lowest concentrations of the samples has made the potential of magnetic nanocarriers for use as antimicrobial agents.

4. Conclusions

The present study presents the synthesis of Fe_3O_4 nanoparticles stabilised with citrate anion and loaded with polyphenols. The magnetite nanoparticles were loaded with biologically active compounds (caffeic acid and gallic acid). The magnetic nanocarriers determined a significant sensitivity on the Gram-positive and Gram-negative bacteria strains and inhibited their growth. Therefore, based on the morphological results, the Fe3O4@citrate@polyphenols nano-drugs represent suitable candidates as antibacterial agents. They can be used for biomedical applications. Further studies will test the suitability of using two antimicrobial agents, one polyphenol and one classic antibiotic and evaluate their synergism.

Acknowledgements:

This work was supported by a grant from the Romanian Ministry of Education and Research, CNCS-UEFISCDI, project number PN-III-P2-2.1-PED-2019-4813 (Exploitation of the magnetic nanoparticles in developing magnetic microdevices) and Proof-of-Concept Project funded by the University POLITEHNICA of Bucharest.

R E F E R E N C E S

[1] M. Radulescu, S. Popescu, D. Ficai, M. Sonmez, O. Oprea, A. Spoială, A. Ficai, E. Andronescu, "Advances in Drug Delivery Systems, from 0 to 3D Superstructures", Curr Drug Targets, **17**, 2016, 1-13.

[2] C. Chircov, R.E. Stefan, G. Dolete, A. Andrei, A.M. Holban, O.C. Oprea, B.S. Vasile, I.A. Neacsu, B. Tihauan, "Dextran-Coated Iron Oxide Nanoparticles Loaded with Curcumin for Antimicrobial Therapies", Pharmaceutics, **14**(5), 2022.

[3] M. Caciandone, A.G. Niculescu, A.R. Rosu, V. Grumezescu, I. Negut, A.M. Holban, O. Oprea, B.S. Vasile, A.C. Birca, A.M. Grumezescu, M.S. Stan, A.G. Anghel, I. Anghel, "PEG-Functionalized Magnetite Nanoparticles for Modulation of Microbial Biofilms on Voice Prosthesis", Antibiotics, **11**(1), 2022, 0039.
[4] M. Caciandone, A.G. Niculescu, V. Grumezescu, A.C. Birca, I.C. Ghica, B.S. Vasile, O. Oprea, I.C. Nica, M.S. Stan, A.M. Holban, A.M. Grumezescu, I. Anghel, A.G. Anghel, "Magnetite Nanoparticles Functionalized with Therapeutic Agents for Enhanced ENT Antimicrobial Properties", Antibiotics-Basel, **11**(5), 2022.
[5] R.A. Puiu, P.C. Balaure, E. Constantinescu, A.M. Grumezescu, E. Andronescu, O.C. Oprea, B.S. Vasile, V. Grumezescu, I. Negut, I.C. Nica, M.S. Stan, "Anti-Cancer Nanopowders and MAPLE-Fabricated Thin Films Based on SPIONs Surface Modified with Paclitaxel Loaded beta-Cyclodextrin", Pharmaceutics, **13**(9), 2021, 1356.
[6] H.B. Mohammed, S.M.I. Rayyif, C. Curutiu, A.C. Birca, O.C. Oprea, A.M. Grumezescu, L.M. Ditu, I. Gheorghe, M.C. Chifiriuc, G. Mihaescu, A.M. Holban, "Eugenol-Functionalized Magnetite Nanoparticles Modulate Virulence and Persistence in Pseudomonas aeruginosa Clinical Strains", Molecules, **26**(8), 2021, 2189.
[7] O. Gherasim, R.C. Popescu, V. Grumezescu, G.D. Mogosanu, L. Mogoanta, F. Iordache, A.M. Holban, B.S. Vasile, A.C. Birca, O.C. Oprea, A.M. Grumezescu, E. Andronescu, "MAPLE Coatings Embedded with Essential Oil-Conjugated Magnetite for Anti-Biofilm Applications", Materials, **14**(7), 2021, 1612.
[8] S. Huang, Y. Chen, B. Liu, F. He, P. Ma, X. Deng, Z. Cheng, J. Lin, "Synthesis of magnetic and upconversion nanocapsules as multifunctional drug delivery system", Journal of Solid State Chemistry, **229**, 2015, 322-329.
[9] A. Gandhi, A. Paul, S.O. Sen, K.K. Sen, "Studies on thermoresponsive polymers: Phase behaviour, drug delivery and biomedical applications", Asian J Pharm Sci, **10**(2), 2015, 99-107.
[10] D. Ficai, O. Oprea, A. Ficai, A.M. Holban, "Metal Oxide Nanoparticles: Potential Uses in Biomedical Applications", Curr Proteomics, **11**(2), 2014, 139-149.
[11] A.G. Sagdicoglu Celep, A. Demirkaya, E.K. Solak, "Antioxidant and anticancer activities of gallic acid loaded sodium alginate microspheres on colon cancer", Current Applied Physics, 2020.
[12] B. Zhou, L.M. Wu, L. Yang, Z.L. Liu, "Evidence for alpha-tocopherol regeneration reaction of green tea polyphenols in SDS micelles", Free radical biology & medicine, **38**(1), 2005, 78-84.
[13] M.E. Cavet, K.L. Harrington, T.R. Vollmer, K.W. Ward, J.Z.Z. Zhang, "Anti-inflammatory and antioxidative effects of the green tea polyphenol epigallocatechin gallate in human corneal epithelial cells.", Molecular Vision, **17**, 2011, 533:542.
[14] L.R. Ferguson, "Role of plant polyphenols in genomic stability", Mutation Research, **475 (1-2)**(89-111), 2001.
[15] K.W. Ong, A. Hsu, L. Song, D. Huang, B.K. Tan, "Polyphenols-rich Vernonia amygdalina shows anti-diabetic effects in streptozotocin-induced diabetic rats", Journal of ethnopharmacology, **133**(2), 2011, 598-607.
[16] L. Xiang, K. Sun, J. Lu, Y. Weng, A. Taoka, Y. Sakagami, J. Qi, "Anti-aging effects of phloridzin, an apple polyphenol, on yeast via the SOD and Sir2 genes", Bioscience, biotechnology, and biochemistry, **75**(5), 2011, 854-8.
[17] C. Locatelli, F.B. Filippin-Monteiro, T.B. Creczynski-Pasa, "Alkyl esters of gallic acid as anticancer agents: a review", European journal of medicinal chemistry, **60**, 2013, 233-9.
[18] S. Verma, A. Singh, A. Mishra, "Gallic acid: molecular rival of cancer", Environmental toxicology and pharmacology, **35**(3), 2013, 473-85.
[19] M.T. Mansouri, B. Naghizadeh, B. Ghorbanzadeh, Y. Farbood, A. Sarkaki, K. Bavarsad, "Gallic acid prevents memory deficits and oxidative stress induced by intracerebroventricular injection of streptozotocin in rats", Pharmacology, biochemistry, and behavior, **111**, 2013, 90-6.
[20] Y. Lu, F. Jiang, H. Jiang, K. Wu, X. Zheng, Y. Cai, M. Katakowski, M. Chopp, S.S. To, "Gallic acid suppresses cell viability, proliferation, invasion and angiogenesis in human glioma cells", European journal of pharmacology, **641**(2-3), 2010, 102-7.

[21] S. Madlener, C. Illmer, Z. Horvath, P. Saiko, A. Losert, I. Herbacek, M. Grusch, H.L. Elford, G. Krupitza, A. Bernhaus, M. Fritzer-Szekeres, T. Szekeres, "Gallic acid inhibits ribonucleotide reductase and cyclooxygenases in human HL-60 promyelocytic leukemia cells", Cancer Lett, **245**(1-2), 2007, 156-62.
[22] S.C. Forester, A.L. Waterhouse, "Gut metabolites of anthocyanins, gallic acid, 3-O-methylgallic acid, and 2,4,6-trihydroxybenzaldehyde, inhibit cell proliferation of Caco-2 cells", J Agric Food Chem, **58**(9), 2010, 5320-7.
[23] Z. Liu, D. Li, L. Yu, F. Niu, "Gallic acid as a cancer-selective agent induces apoptosis in pancreatic cancer cells", Chemotherapy, **58**(3), 2012, 185-94.
[24] N. Nayeem, A. Smb, "Gallic Acid: A Promising Lead Molecule for Drug Development", Journal of Applied Pharmacy, **08**(02), 2016.
[25] I. Gulcin, "Antioxidant activity of caffeic acid (3,4-dihydroxycinnamic acid)", Toxicology, **217**(2-3), 2006, 213-20.
[26] N.J. Kang, K.W. Lee, B.J. Shin, S.K. Jung, M.K. Hwang, A.M. Bode, Y.S. Heo, H.J. Lee, Z. Dong, "Caffeic acid, a phenolic phytochemical in coffee, directly inhibits Fyn kinase activity and UVB-induced COX-2 expression", Carcinogenesis, **30**(2), 2009, 321-30.
[27] K.C. Liu, H.C. Ho, A.C. Huang, B.C. Ji, H.Y. Lin, F.S. Chueh, J.S. Yang, C.C. Lu, J.H. Chiang, M. Meng, J.G. Chung, "Gallic acid provokes DNA damage and suppresses DNA repair gene expression in human prostate cancer PC-3 cells", Environmental toxicology, **28**(10), 2013, 579-87.
[28] H.M. Chen, Y.C. Wu, Y.C. Chia, F.R. Chang, H.K. Hsu, Y.C. Hsieh, C.C. Chen, S.S. Yuan, "Gallic acid, a major component of Toona sinensis leaf extracts, contains a ROS-mediated anti-cancer activity in human prostate cancer cells", Cancer Lett, **286**(2), 2009, 161-71.
[29] A.A. Abd Elrahman, F.R. Mansour, "Targeted magnetic iron oxide nanoparticles: Preparation, functionalization and biomedical application", J Drug Deliv Sci Tec, **52**, 2019, 702-712.
[30] M. Barrow, A. Taylor, A.M. Fuentes-Caparros, J. Sharkey, L.M. Daniels, P. Mandal, B.K. Park, P. Murray, M.J. Rosseinsky, D.J. Adams, "SPIONs for cell labelling and tracking using MRI: magnetite or maghemite?", Biomater Sci, **6**(1), 2017, 101-106.
[31] T. Zare, N. Sattarahmady, "A Mini-Review of Magnetic Nanoparticles: Applications in Biomedicine", Basic & Clinical Cancer Research, **7**(4), 2015, 29-39.
[32] C. Tapeinos, "Magnetic Nanoparticles and Their Bioapplications", 2018, 131-142.
[33] I. Negut, V. Grumezescu, Chapter 3 - Nanoparticles and hyperthermia, in: A.M. Grumezescu (Ed.), Biomedical Applications of Nanoparticles, William Andrew Publishing2019, pp. 63-90.
[34] E.D. Teodor, F. Gatea, A. Ficai, G.L. Radu, "Functionalized Magnetic Nanostructures for Anticancer Therapy", Curr Drug Targets, **19**(3), 2018, 239-247.
[35] L.S. Arias, J.P. Pessan, A.P.M. Vieira, T.M.T. Lima, A.C.B. Delbem, D.R. Monteiro, "Iron Oxide Nanoparticles for Biomedical Applications: A Perspective on Synthesis, Drugs, Antimicrobial Activity, and Toxicity", Antibiotics, **7**(2), 2018.
[36] N. Ajinkya, X. Yu, P. Kaithal, H. Luo, P. Somani, S. Ramakrishna, "Magnetic Iron Oxide Nanoparticle (IONP) Synthesis to Applications: Present and Future", Materials (Basel), **13**(20), 2020.
[37] I.M. Vlad, D.C. Nuță, R.V. Ancuceanu, M.T. Caproiou, F. Dumitrascu, I.C. Marinas, M.C. Chifiriuc, L.G. Măruțescu, I. Zarafu, I.R. Papacocea, B.Ș. Vasile, A.I. Nicoară, C.-I. Ilie, A. Ficai, C. Limban, "New O-Aryl-Carbamoyl-Oxymino-Fluorene Derivatives with MI-Crobicidal and Antibiofilm Activity Enhanced by Combination with Iron Oxide Nanoparticles", Molecules, **26**(10), 2021, 1-19.
[38] A. Spoiala, C.I. Ilie, R.D. Trusca, O.C. Oprea, V.A. Surdu, B.S. Vasile, A. Ficai, D. Ficai, E. Andronescu, L.M. Ditu, "Zinc Oxide Nanoparticles for Water Purification", Materials, **14**(16), 2021, 4747-4763.
[39] CLSI, Performance Standards for Antimicrobial Susceptibility Testing. CLSI supplement M100, 31st ed., Clinical and Laboratory Standards Institute, USA, 2021.

[40] R. Roto, A. Izza, E.S. Kunarti, S. Suherman, "Effect of Stabilizing Agent of Sodium Citrate and Polyethylene Glycol on Structure of Fe₃O₄ Nanoparticles", Key Engineering Materials, **840**, 2020, 466-471.
[41] S. Nigam, K.C. Barick, D. Bahadur, "Development of citrate-stabilized Fe3O4 nanoparticles: Conjugation and release of doxorubicin for therapeutic applications", J Magn Magn Mater, **323**(2), 2011, 237-243.
[42] A. Saraswathy, S.S. Nazeer, M. Jeevan, N. Nimi, S. Arumugam, V.S. Harikrishnan, P.R. Varma, R.S. Jayasree, "Citrate coated iron oxide nanoparticles with enhanced relaxivity for in vivo magnetic resonance imaging of liver fibrosis", Colloids Surf B Biointerfaces, **117**, 2014, 216-24.
[43] S. Machmudah, W. Wahyudiono, H. Kanda, M. Goto, "Synthesis of Polyhedral Magnetite Particles by Hydrothermal Process under High Pressure Condition", Journal of Engineering and Technological Sciences, **48**(6), 2016, 753-771.
[44] S. Srivastava, R. Awasthi, N.S. Gajbhiye, V. Agarwal, A. Singh, A. Yadav, R.K. Gupta, "Innovative synthesis of citrate-coated superparamagnetic Fe3O4 nanoparticles and its preliminary applications", J Colloid Interface Sci, **359**(1), 2011, 104-11.
[45] D. Ficai, E. Andronescu, A. Ficai, G. Voicu, B. Vasile, V. Ionita, C. Guran, "Synthesis and Characterization of Mesoporous Magnetite Based Nanoparticles", Curr Nanosci, **8**(6), 2012, 875-879.
[46] B.K. Sodipo, A. Abdul Aziz, "Non-seeded synthesis and characterization of superparamagnetic iron oxide nanoparticles incorporated into silica nanoparticles via ultrasound", Ultrason Sonochem, **23**, 2015, 354-9.
[47] R.G. RuizMoreno, A.I. Martinez, R. Castro-Rodriguez, P. Bartolo, "Synthesis and Characterization of Citrate Coated Magnetite Nanoparticles", J Supercond Nov Magn, **26**(3), 2012, 709-712.
[48] S.T. Shah, A.Y. W, O. Saad, K. Simarani, Z. Chowdhury, A.A. A, L.A. Al-Ani, "Surface Functionalization of Iron Oxide Nanoparticles with Gallic Acid as Potential Antioxidant and Antimicrobial Agents", Nanomaterials (Basel), **7**(10), 2017.
[49] D. Dorniani, M.Z. Hussein, A.U. Kura, S. Fakurazi, A.H. Shaari, Z. Ahmad, "Preparation of Fe(3)O(4) magnetic nanoparticles coated with gallic acid for drug delivery", Int J Nanomedicine, **7**, 2012, 5745-56.
[50] V.A. Spirescu, A.G. Niculescu, S. Slave, A.C. Birca, G. Dorcioman, V. Grumezescu, A.M. Holban, O.C. Oprea, B.S. Vasile, A.M. Grumezescu, I.C. Nica, M.S. Stan, E. Andronescu, "Anti-Biofilm Coatings Based on Chitosan and Lysozyme Functionalized Magnetite Nanoparticles", Antibiotics-Basel, **10**(10), 2021, 1269.
[51] C. Chircov, M.F. Matei, I.A. Neacsu, B.S. Vasile, O.C. Oprea, A.M. Croitoru, R.D. Trusca, E. Andronescu, I. Sorescu, F. Barbuceanu, "Iron Oxide-Silica Core-Shell Nanoparticles Functionalized with Essential Oils for Antimicrobial Therapies", Antibiotics, **10**(9), 2021, 1138.
[52] N.B. Saleh, B. Chambers, N. Aich, J. Plazas-Tuttle, H.N. Phung-Ngoc, M.J. Kirisits, "Mechanistic lessons learned from studies of planktonic bacteria with metallic nanomaterials: implications for interactions between nanomaterials and biofilm bacteria", Front Microbiol, **6**, 2015, 677.
[53] S. Saqib, M.F.H. Munis, W. Zaman, F. Ullah, S.N. Shah, A. Ayaz, M. Farooq, S. Bahadur, "Synthesis, characterization and use of iron oxide nano particles for antibacterial activity", Microsc Res Tech, **82**(4), 2019, 415-420.
[54] L. Gabrielyan, H. Badalyan, V. Gevorgyan, A. Trchounian, "Comparable antibacterial effects and action mechanisms of silver and iron oxide nanoparticles on Escherichia coli and Salmonella typhimurium", Sci Rep, **10**(1), 2020, 13145.
[55] R.A. Ismail, G.M. Sulaiman, S.A. Abdulrahman, T.R. Marzoog, "Antibacterial activity of magnetic iron oxide nanoparticles synthesized by laser ablation in liquid", Materials science & engineering. C, Materials for biological applications, **53**, 2015, 286-97.